ISSN 0020-4412, Instruments and Experimental Techniques, 2015, Vol. 58, No. 2, pp. 181–189. © Pleiades Publishing, Ltd., 2015.
Original Russian Text © M.I. Bryzgunov, A.D. Goncharov, V.M. Panasyuk, V.V. Parkhomchuk, V.B. Reva, D.N. Skorobogatov, 2015, published in Pribory i Tekhnika Eksperimenta, 2015, No. 2, pp. 14–23.

NUCLEAR EXPERIMENTAL TECHNIQUES

Energy Transfer in the High-Voltage Electron Cooler for the COSY Synchrotron Ring

M. I. Bryzgunov, A. D. Goncharov, V. M. Panasyuk, V. V. Parkhomchuk, V. B. Reva*, and D. N. Skorobogatov

Budker Institute of Nuclear Physics, Siberian Branch, Russian Academy of Sciences, pr. Akademika Lavrent'eva 11, Novosibirsk, 630090 Russia

** e-mail: V.B.Reva@inp.nsk.su*

Received May 30, 2014

Abstract—An electron cooler produced by the Budker Institute of Nuclear Physics was put into operation at the COSY synchrotron (Jülich, Germany) in 2013. This electron cooler has been designed for suppressing the effect of beam scattering by an internal target at energies as high as the maximum proton beam energy of 3 GeV. As the electron cooler was developed, many complicated electrotechnical problems were solved. One of these problems was the transfer of the electric power to many electronic consumers kept at a high electric potential. Several practical methods for solving this problem are described. These variants were analyzed and tested while designing the cooler construction. The final decision is based on the principle of operation of the cascade transformer containing 33 sections connected in series. The described design solutions can be used not only for future electron coolers in projects NICA-JINR (Dubna, Russia), FAIR (Germany), and MEIC (United States), but also for other high-voltage facilities requiring power transfer to devices held at a high potential. After decommissioning of the electron cooler at Fermilab (United States), the described facility has become the highest-voltage electron cooler worldwide.

DOI: 10.1134/S0020441215020165

INTRODUCTION

In operation of electrostatic partide accelerators accelerators, it is often required that electric power be transferred to devices kept at a potential as high as a few megavolts. There are several methods for solving this problem. Let us consider some of them with reference to electron cooling facilities.

Power transfer systems embodying the transformer principle are used, as a rule, in facilities at a voltage as high as 300 kV. These are either ordinary electrotechnical transformers with reinforced insulation between the windings disposed on a common magnetic core [1] or transformers with a large gap between the windings in which the magnetic flux travels a portion of its path beyond the magnetic core in the insulating medium (oil or sulfur hexafluoride) [2, 3]. A similar design was used for the prototype of the 1-MV SILUET electron cooler [4]. Nevertheless, at a high intensity of scattered fields and a low converter frequency, problems arise with the attaining of a high stability of the high voltage, which is required for the electron cooling (10^{-4} or better).

A mechanical link of motor – nonconducting shaft – electric motor–generator was used in the electron cooling facility at Fermilab (United States) [5]. This system allowed power transfer at a potential of up to 4.3 MV.

Several methods were considered when designing the power transfer system for the 2-MeV electron cooling facility (COSY, Germany) with allowance for its specific features. The specific features consisted in the necessity to supply power not only for the high-voltage terminal, but also for numerous isolated sections (a total of 34) containing electronics for establishing a homogeneous magnetic field along the accelerating tube and high-voltage rectifiers for generating the high voltage. The characteristic values of the powers are 5–10 kW for the high-voltage terminal and ~300 W per section. The need for a great number of sections results from the rigid requirements for operation with electron beam in range from 25 keV to 2 MeV. Under these conditions, it is extremely difficult to form the electron beam optics similar to the optics used by the Fermilab in [6], which was mostly oriented for a fixed energy. A relatively small number of solenoids used as the magnetic focusing elements were included in the optical channel of the accelerating column at Fermilab. Preliminary examination of the variant with the use of a nonconducting shaft for power transfer between numerous sections has revealed significant engineering difficulties with the fastening of the shaft

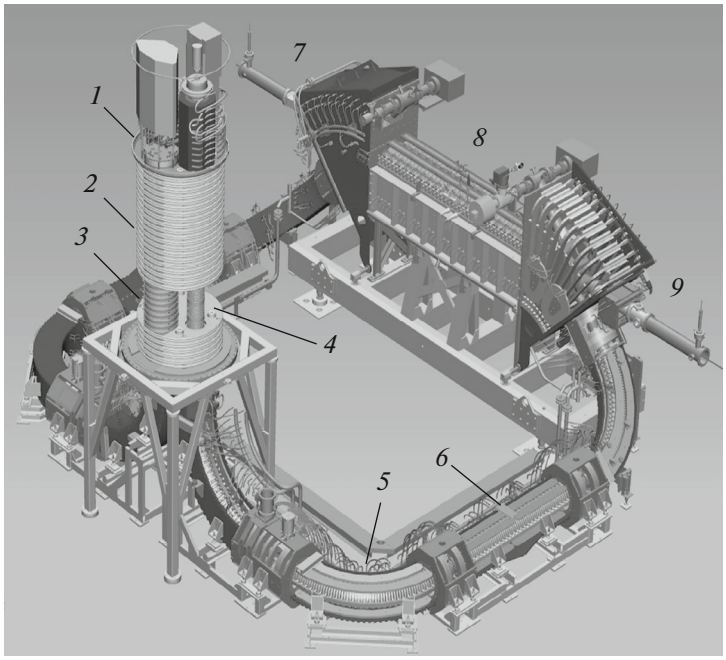

Fig. 1. Three-dimensional model of the 2-MeV electron cooling system for the COSY accelerator: (*1*) high-voltage terminal containing an electron gun, a collector, and electronics; (*2*) high-voltage sections; (*3*) cascade transformer; (*4*) accelerating tube; (*5*) bending solenoids of the transport beamline; (*6*) straight-line solenoids of the transport beamline; (*7*) toroids; (*8*) cooling section; and (*9*) transport beamline for the ion beam.

and the generator, mechanical stresses and vibrations [5] appearing between the sections, passage of the shaft through the section, initial settings, and assembling of the entire system.

A 2-MeV ELECTRON COOLER

An electron cooling facility for electron energies ranging to 2 MeV was developed in 2009–2012 by the Budker Institute of Nuclear Physics (BINP) for the COSY synchrotron [7, 8]. The COSY synchrotron has been designed for experiments with polarized and nonpolarized protons in the energy range of up to 2600 MeV at the internal target or with the beam extraction to the external target. The possibility of "cooling" the used beam (i.e., reducing the spread in the particle momentum) with the aim of suppressing the "heating" effects is very important for experiments with the internal target. The electron cooling method is based on the "heat exchange" between the ion beam circulating in the storage ring and the electron beam moving with the same average velocity. "Hot" protons are cooled by Coulomb collisions in the gas of "cold" electrons on the common portion of the trajectory in the rest of the frame of the beams. The cooling process lasts until the proton temperature in the center-of-mass system becomes equal to the effective temperature.

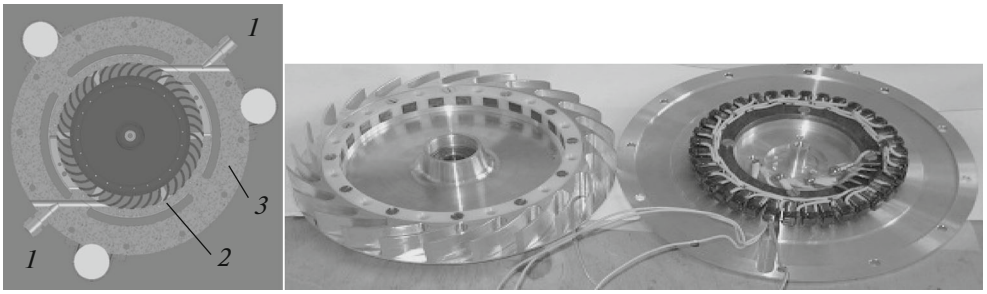

(a) (b)

Fig. 2. (a) Design and (b) external appearance of the pneumatic generator: (*1*) nozzle for supplying gas, (*2*) rotor of the pneumatic generator, and (*3*) element of the casing.

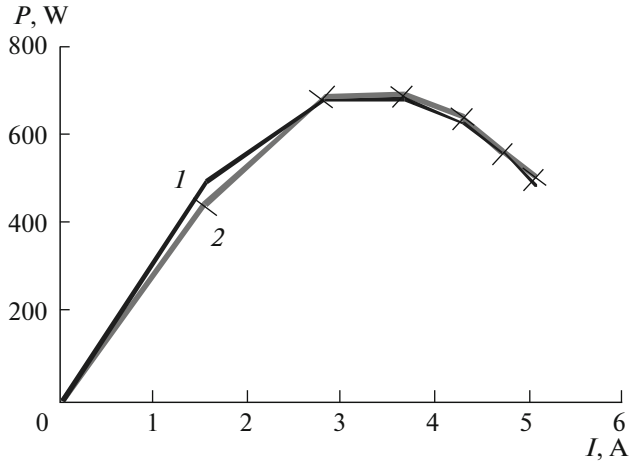

Fig. 3. Dependence of the power supplied by the generator on the load current: (*1*) load current for the generator with a maximum voltage of 420 V and an intrinsic resistance of 65 Ω, and (*2*) measured values.

The layout of the electron cooling facility is shown in Fig. 1. The devices of the electron gun and the collector are located at the vertex of the accelerator in the high-voltage terminal *1* at a potential of up to 2 MV. The stationary electron beam with a current as high as a few amperes is accelerated along the electrostatic column consisting of high-voltage sections *2* and, afterward, is guided over the transport system toward cooling section *8*, where it moves jointly with ion beam *9*. The joint motion results in transferring the heat energy from hotter ions to colder electrons. After leaving the cooling section, the electron beam returns and, moving over the transport channel, reaches the column again, where it loses almost all the accumulated energy and is absorbed by the collector. In its trajectory, the beam is always located in the guiding magnetic field. All components of the electrostatic accelerator (*1*–*4*) are placed in a tank with high-pressure sulfur hexafluoride gas.

The 2-MeV direct-action electrostatic accelerator consists of 33 identical sections (*2*), each of which contains two magnetic coils for focusing the accelerated and decelerated beams, a high-voltage unit for generating a high voltage of 60 kV between the sections, and a module for control and communication. Each section is powered from its own supply in the form of a cascade transformer section.

A PNEUMATIC GENERATOR

One of the proposals for energy transfer under a high potential was based on the use of a compressed gas. In comparison with the use of an shaft, it simplifies substantially the system for supplying power for a specific section, eliminates the rigid requirements for the accuracy of generator fastening, and improves essentially the situation with mechanical vibrations, since the rotation speed of the pneumatic turbine may be rather high, and the rigid mechanical link between sections is absent.

The construction of the electric pneumatic generator produced by the BINP is shown in Fig. 2. The pneumatic generator consists of a stator with 36 coils fixed in positions on it, and a rotor with 24 permanent magnets. The coils are serially connected in three groups, so that the generator produces three-phase ac voltage. The rated generator frequency depends on the load and is ~2 kHz. The specific frequency value has not been so significant, since the powered electronics contains the voltage changer with preliminary rectification. The high frequency of the ac voltage encourages the obtaining of the stable supply voltage for the electronic modules of the high-voltage section. This pneumatic generator was tested at an operating inlet pressure of 4.6 atm, and air was the actuating medium. Two 4-mm-diameer nozzles were used to create a gas flow. The voltage of the free-running generator was 400 V. The maximum power of ~600 W was attained at a load of 65 Ω, and, in this case, the voltage was 200 V. The generator occupied 4 cm in height.

The gas flow from the nozzle can be estimated by the formula in [9] for atmospheric air in the case when the back pressure is $p_2 < 0.5p$:

$$S = 0.38F\frac{p}{\sqrt{T}}, \quad (1)$$

where F [cm^2] is the nozzle cross section, p [kilogram-force/cm^2] is the pressure, and T is the absolute temperature in the pressure tank. Under nominal conditions, the gas flow rate is $S = 0.031$ kg/s.

When estimating the energy expediency, one must take into account that it is for the energy transfer that this system is intended. Therefore, nominally, it is possible to utilize the energy of an expanding gas that has not been used for turbine rotation. If the standard approach is used to obtain compressed gas, the gas is isothermally or adiabatically compressed in the compressor, and the excess heat is removed from the actuating medium. In this case, losses due to work on the obtaining of a compressed gas appear even if an ideal compressor is employed. Under the perfect compressor, we mean a compressor that has zero energy losses in its valves, gas leaks, and flow-over through looseness, and the friction force is zero.

If heat is not removed during adiabatic compression and the hot gas obtained thereby is used to rotate the turbine, the energy loss per thermodynamic cycle can be minimized. However, questions arise related to

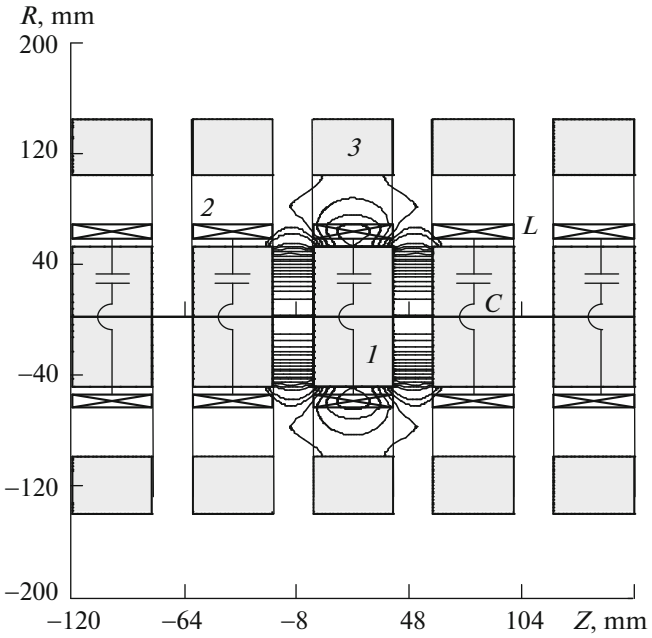

Fig. 4. Diagram of the serial power transfer on large-gap transformers: (*1*) magnetic core transferring the magnetic flux from section to section, (*2*) coil, and (*3*) magnetic core reducing the magnetic flux beyond the transformer; (*1–3*) form inductance L containing intrinsic inductance L_0 (the magnetic flux remains within the section) and coupling inductance L_1 (the magnetic flux is transferred from section to section); and (*C*) capacitor of the oscillating loop.

the operation of the entire gas system at high temperatures. For the turbine proper, this engineering problem can be solved by selecting materials and design, but, for the gas transport system, it may be significant. Since the turbine is held at a high potential, elements of the gas transport system must be produced from dielectric and, desirably, flexible material.

The first variant was used in these experiments, since the estimated gas temperature upon adiabatic compression was 200°C (the adiabatic index for air was assumed to be 1.4). The dependence of the power supplied by the pneumatic generator on the load current is presented in Fig. 3. The work spent on the actuator of the ideal compressor during isothermal compression can be estimated by formula [10]

$$A = \frac{S}{\mu} RT \ln\left(\frac{p_2}{p_1}\right) = 4.6 \text{ kW}, \qquad (2)$$

where μ is the molar mass of air, R is the gas constant, and p_2 and p_1 are the inlet and outlet compressor pressures. The power transfer efficiency appears to be at a level of 10%.

A similar turbine has been used for a few years at the Accelerator Mass Spectrometer setup of the BINP [11] for powering elements of the high-voltage terminal being at a potential of 1 MV. The actuating medium is air, since it is easy to use. The insulating medium is air with a small admixture of sulfur hexafluoride gas added in proportion of 2–3%. Initially, frequent failures happened through loss of the oil lubricant from the bearing. After refinement of the design that has eliminated oil losses, the facility is capable of continuously operating for more than two years with 12-h work in labor days. One of the problems encountered in its use was the excessive cooling of the gas transport system tubing upon gas expansion in the pneumatic generator, which necessitated additional monitoring of the humidity content of the insulating gas with the aim of avoiding condensate production and artificial gas heating past the compressor. Cross-linked polyethylene tubing was used as the gas transport system.

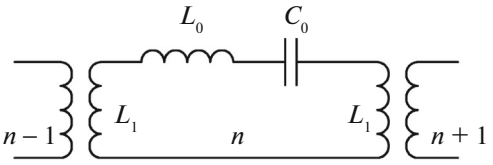

Fig. 5. Diagram of power transfer on a series of large-gap transformers.

The use of sulfur hexafluoride as the actuating medium of the pneumatic generator may offer a chance to proceed to the second variant. Since the reference value of the adiabatic index is 1.1, the temperature after adiabatic compression is expected to be at a level of 70°C, which seems to be acceptable from the engineering standpoint. The use of sulfur hexafluoride as a high-voltage insulating medium provides an additional advantage, which consists in specifying looser requirements for the gas transport system hermeticity.

Though the pneumatic generator has been used to good effect, this engineering solution has not been selected for designing the electron cooler for our setup due to the technological difficulties on maintaining continuous operation of numerous sections over a long period of time.

A CASCADE TRANSFORMER WITH A LARGE GAP

The central core can be excluded from the transformer design to ensure good insulation between the transformer windings. Such design is used in ELV-type high-voltage accelerators [12], EC-300 electron cooler [2], etc. For power to be supplied for numerous sections, this idea may be extended by using a great number of identical sections transferring energy based on the running wave principle. The construction is

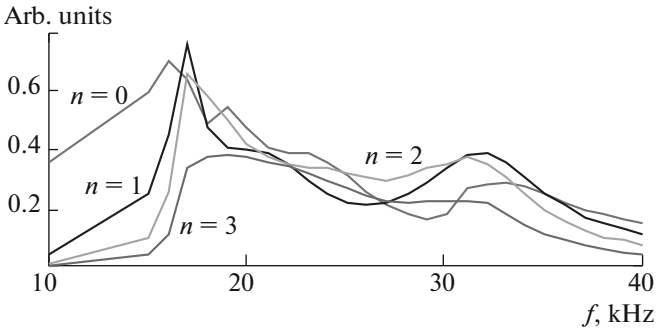

Fig. 6. Frequency dependence of the voltage applies to the sections.

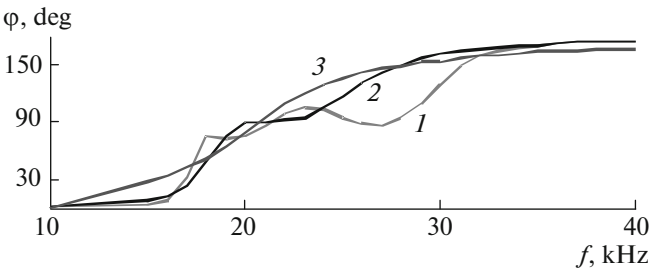

Fig. 7. Dependence of the phase shift on the frequency between adjacent sections: (*1*) phase shift between sections $n = 0$ and 1, (*2*) $n = 1$ and 2, and (*3*) $n = 2$ and 3. When $\omega = \omega_0$ and the reflected wave is absent, this corresponds to φ from Eq. (4).

schematically shown in Fig. 4. Inductance element L consists of magnetic core section *1* with coil *2* wound over it. Together with capacitor C, it forms an elementary oscillating loop.

The cell coupling is effected by the magnetic flux. It is assumed that only adjacent cells are coupled, and the coupling via the cell is negligible. For the excitation of vortex electric fields by the scattered magnetic fields to be minimized, each cell is placed in the external element of the magnetic core *3*.

The equivalent circuit diagram of this system is shown in Fig. 5, where L_1 is the coupling inductance, C_0 is the capacitor of the elementary oscillating loop, L_0 is the intrinsic inductance, and R_0 is the resistance of the equivalent losses.

The Kirchhoff equation for an elementary cell can be written as follows:

$$L_0 \frac{dI_n}{dt} + R_0 I_n + \frac{q_n}{C_0} = L_1 \frac{dI_{n-1}}{dt} + L_1 \frac{dI_{n+1}}{dt}, \qquad (3)$$

where n is the serial number of the cell, and q_n is charge at the capacitor C_0. At $R_0 = 0$, this equation admits solution in the form of the running wave:

$$I_n = I_0 \exp(-i\omega t) \exp(in\varphi), \qquad (4)$$

provided that

$$\cos\varphi = \frac{1}{2}\frac{L_0}{L_1}\left(1 - \frac{\omega_0^2}{\omega^2}\right), \quad -1 < \cos\varphi < 1,$$
$$\frac{\omega_0^2}{1 + 2\dfrac{L_1}{L_0}} < \omega^2 < \frac{\omega_0^2}{1 - 2\dfrac{L_1}{L_0}}, \qquad (5)$$

where $\omega_0^2 = \dfrac{1}{L_0 C_0}$, and φ is the phase shift between adjacent sections.

The power flow can be estimated by the formula

$$S_0 = \omega L_1 I_0^2 \sin\varphi. \qquad (6)$$

It is apparent that it increases linearly with increase in the frequency and coupling inductance, reaching its maximum at resonant frequency $\omega = \omega_0$, when the phase shift between the sections is $\varphi = \pi/2$.

The decrease in the voltage amplitude from section to section is described by decrement

$$\delta = \frac{\gamma}{2\omega_0}\frac{L_0}{L_1}\frac{1}{\sin\varphi}, \qquad (7)$$

where $\gamma = R_0/L_0$.

It is apparent that, for the high-quality power transfer to a greater number of sections (~30) to be ensured, the Q factor of the elementary oscillating loop must be maintained at a high level ($Q = \gamma/\omega_0 \sim 100$), which is a complex engineering problem. The other engineering problem is the necessity to maintain the load resistance equal to wave impedance of the link $\rho = L_1\omega_0$, where L_1 is the coupling inductance. If the impedance departs from this value, reflected waves appear, which has a negative effect on the distribution of the voltage among the sections.

A four-section experimental model has been produced. The parameters of its elements are as follows: $L_0 = 0.58$ mH, the coupling factor between sections $L_1/L_0 = 0.44$, the resonant frequency of the unit loop $f_0 = 21$ kHz, and its Q factor $Q = 34$. The load resistance (25 Ω) is equal to the wave impedance of the link at the resonant frequency. The frequency dependence of the amplitude of oscillations is shown in Fig. 6 for different sections n, and the voltage phase shift between adjacent sections is presented in Fig. 7. It is apparent that, at a frequency of 21 kHz, the currents in adjacent sections are shifted by 90°, and the voltage amplitudes in different sections are approximately equal, thus corresponding to the case of the running wave. The decrease in the voltage amplitude from section to section is in good agreement with formula (7).

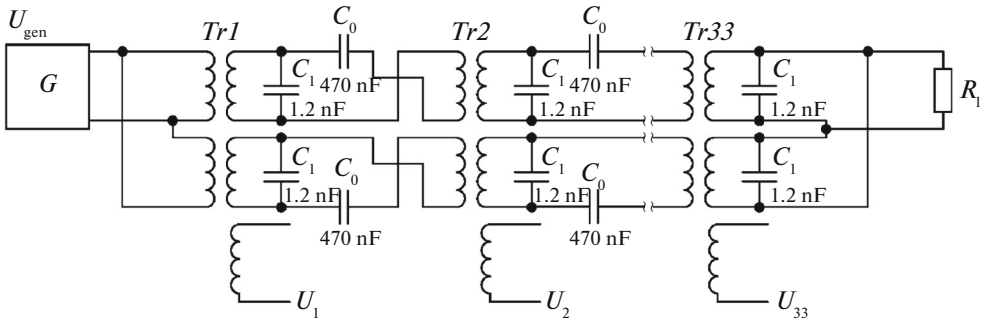

Fig. 8. Circuit diagram of the cascade transformer.

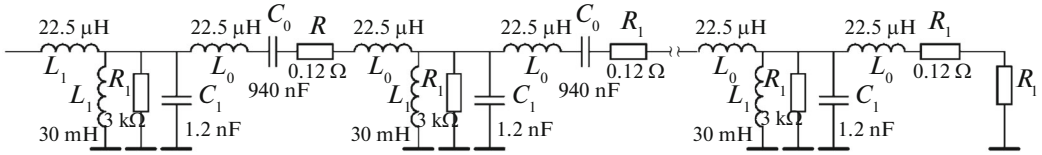

Fig. 9. Equivalent circuit diagram of the cascade transformer.

Therefore, this idea has the right for existence, but everything is complicated by the engineering problems with the development of technologically feasible higher-power elementary oscillators with a greater Q factor. Among the advantages of this scheme is the possibility of attaining good high-voltage insulation among the sections, since they do not have common electric components.

A CASCADE TRANSFORMER

A more traditional approach consists in developing a cascade transformer based on an ordinary transformer with a common magnetic core. In this case, a high-quality coupling between adjacent transformers and a low scattering induction is obtained. Nevertheless, the necessity arises to guarantee the high-voltage insulation between the primary and secondary windings, as well as their isolation from the magnetic core. In this case, the scattering induction, though being considerably lower, remains high enough to call for the compensating capacitors. It is this scheme that has been selected for implementation in the 2-MeV COSY electron cooler. The key technical requirements for the cascade transformer are as follows: transfer of a 300-W power for each of the 33 sections and power transfer of about 5–10 kW for the high-voltage terminal. The high-voltage sections form the accelerating column with voltages relative to each other from 0.1 to 60 kV. At the vertex of the accelerating column, there is the high-voltage terminal at a potential from 5 kV to 2 MV relative to the earth.

The electrotechnical and equivalent circuit diagrams are shown in Figs. 8 and 9. It is apparent that the voltage value at the final load strongly depends on the scattering induction L_1 and induction in the free-running mode L_0. To increase the voltage transfer ratio of the transformer, the circuit is complemented with capacitors C_0 (Fig. 8), which lower the "short-circuit" impedance at the resonant frequency, and capacitors C_1, which increase the "free-running mode" impedance. The resistors in the equivalent circuit (Fig. 9) correspond to the losses in the magnetic core and in the cascade transformer winding. The resistances were estimated based on the results of investigation of amplitude-frequency characteristic.

The transformer construction shown in Fig. 10 has been made by analogy with the construction of the accelerating tube. The transformer consists of alternating ceramic and metal rings. Inside a metal ring, there is a magnetic core with five windings. One pair of windings is used to transfer the power upward, the other pair is used for communication with the lower transformer, and the fifth winding serves power take-off for the high-voltage section. Each section is equipped with a discharger, so that, in case of high-voltage breakdown, the charge passes through them rather than through the construction of the cascade transformer. The potential of the cascade transformer section is specified by the corresponding potential of

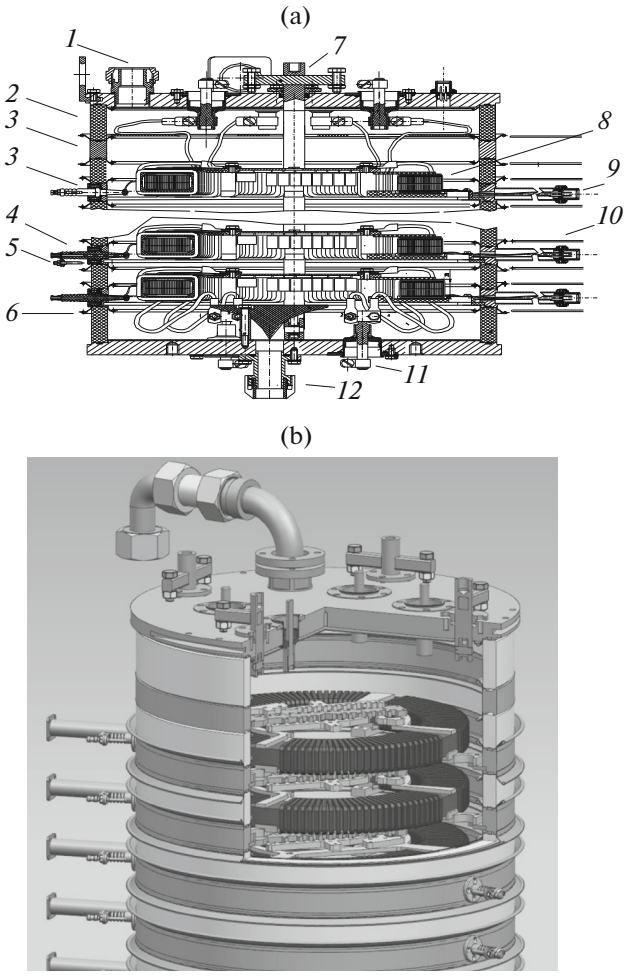

Fig. 10. (a) Outline of the cascade transformer: (*1*) cooling oil outlet, (*2*) ceramic ring, (*3*) metal ring, (*4*) input of the high voltage into the cascade transformer, (*5*) high-voltage discharger, (*6*) guard rings, (*7*) cascade transformer tightening mechanism, (*8*) cascade transformer section, (*9*) output of the power takeoff windings, (*10*) metal surfaces of the high-voltage section in which the power is taken off, (*11*) power input at the ground potential, (*12*) oil outlet, and (b) external appearance of the cascade transformer.

the high-voltage section for which it acts as the power source. Transformer oil is pumped from the bottom to the top to cool the transformer. The oil descends from the top over a special tube made of cross-linked polyethylene. The total length of the cascade transformer is 2.2 m, and the column diameter is 0.4 m. All sections of the cascade transformer are tightened together by means of Kevlar filaments. The key parameters of the cascade transformer are as follows: geometrical size (the outer and inner diameters), ∅28 cm and ∅20 cm; thickness (two 1-cm-thick rings put together), 2 cm; iron mass, 4.8 kg; operating magnetic induction, 2 kG; magnetic loss at an induction of 2.0 kG, 12 W/kg; operating current, up to 35 A (per one branch); total current, up to 70 A; operating voltage, up to 600 V; total power in the transformer, up to 40 kW; total losses, up to 7 kW; number of loops in the power winding (one branch), 28; copper mass, 230 g (28 loops); total copper mass for 4 windings, 1 kg; cross section of the power winding wire (AWG38 RF cable), 5.8 mm^2; and resistance of a single winding at 0 Hz (28 loops), 15 mΩ.

As a magnetic core, we used rings of 5BDSR nanocrystalline iron—a nanocrystalline soft magnetic alloy, which is a new material obtained by fast hardening of a melt on the surface of a rapidly rotating cooling drum. Its advantages are the high induction at a low coercive force, the low remagnetization loss at high frequencies, almost zero magnetostriction, the high magnetic permeability, and the high specific resistance. The effective cross section of the magnetic core is 5.6 cm^2, and the space factor of the magnetic core is 0.7. The magnetic core is impregnated with LBS-1 Bakelite lacquer and has an outer insulation 0.1 mm thick made from a one layer of a nylon film with an overlap ratio of 1.5. To reduce the loss in the force windings associated with a high frequency, they were produced from an AWG-38D litz cable containing 735 0.1-mm-diameter wires.

Figure 11 presents amplitude–frequency characteristics for the equivalent schemes of a short circuit and the free-running mode for the cascade transformer composed of 33 sections. It is apparent that, using the compensating capacitors, we succeeded in obtaining the resonance operating frequencies at a level of 25 kHz. This frequency has been selected as a trade-off between the desire to increase the frequency to the maximum degree with the aim of increasing the energy transfer efficiency and the possibility of encountering problems caused by high-frequency parasitic resonances on an interturn self-capacitance. These problems were observed in the cascade transformer construction described in [13] and did not allow it to reach its rated parameters. Experimental investigation of the amplitude–frequency characteristics for our design demonstrated the presence of parasitic resonances in the frequency range of ~60 kHz.

The voltage distribution along the cascade transformer on the operating electron cooling facility is shown in Fig. 12. Section 10 corresponds to the initial section of the cascade transformer near the generator supplying power for the accelerator, section 42 corresponds to the topmost section near the high-voltage terminal, and sections 0–9 correspond to the power supplies located inside the high-voltage terminal. It is apparent that the obtained voltage distribution over the high-voltage sections is uniform with a high degree of accuracy. The voltage drop between sections is within the limits of the range of the normal performance of the electronic modules.

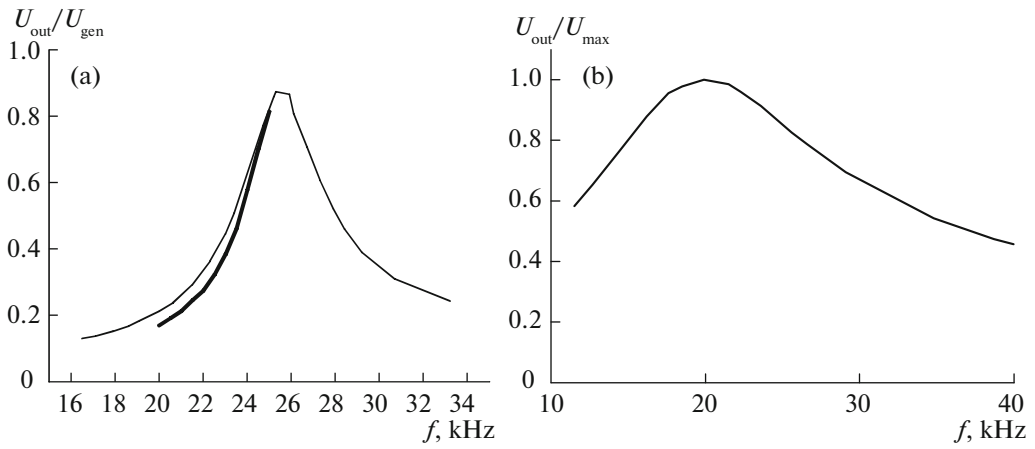

Fig. 11. Amplitude–frequency characteristics (a) of the serial and (b) parallel oscillating loops. The light line corresponds to the values measured at a low voltage (an audio-frequency oscillator), and the heavy line presents the results obtained using a power pulser (30-A current); $R_l = 20\ \Omega$.

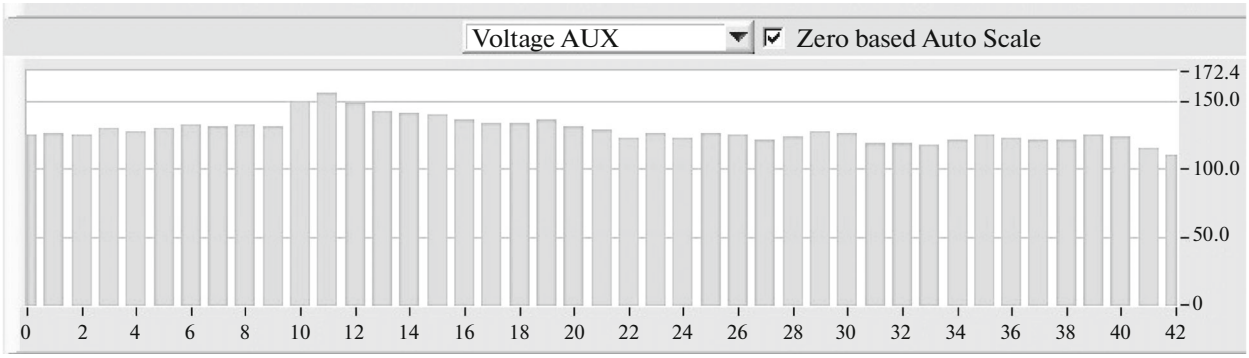

Fig. 12. Distribution of the auxiliaries voltage along the accelerating column.

CONCLUSIONS

The experiments and the practical application of the cascade transformer for supplying power for a great number of sections have demonstrated the feasibility and expediency of this design solution. Nevertheless, experience shows that this solution is close to its practical limit on the length of the cascade transformer and the number of sections. Further increase in the parameters of the cascade transformer (i.e., increase in the number of sections and the maximum potential) calls for new engineering solutions.

REFERENCES

1. Behtenev, E., Bocharov, V., Bubley, V., Vedenev, M., Voskoboinikov, R., Goncharov, A., Evtushenko, Yu., Zapiatkin, N., Zakhvatkin, M., Ivanov, A., Kokoulin, V., Kolmogorov, M., Kondaurov, V., Konstantinov, S., Krainov, G., Kozak, V., Kruchkov, A., Kuper, E., Medvedko, A., Mironenko, L., Panasiuk, V., Parkhomchuk, V., Reva, V., Skrinsky, A., Smirnov, B., Skarbo, B., Sukhina, B., Shrainer, K., Yang, X.D., Zhao, H.W., Li, J., Lu, W., Mao, L.J., Wang, Z.X., Yan, H.B., Zhang, W., and Zhang, J.H., *Proc. RUPAC XIX,* Dubna, Russia, 2004, p. 506.
2. Veremeenko, V.M., Voskoboynikov, R.V., Goncharov, A.D., Evtushenko, Yu.A., Kolmogorov, V.V., Kondaurov, M.N., Kraynov, G.S., Kryuchkov, A.M., Medvedko, A.S., Parkhomchuk, V.V., Petrov, S.P., Reva, V.B., Tiunov, M.A., and Karymov, B.R., *Proc. RUPAC XX,* Novosibirsk, Russia, 2006, p. 97.
3. Valyaev, Yu.D., Kazarezov, I.V., Kuznetsov, V.I., and Ostanin, V.P., *Preprint, of Inst. of Nuclear Phys., Siber. Branch Russ. Acad. Sci.*, Novosibirsk, 1989, no. 89-160.
4. Veis, M.E., Korabelnikov, B.M., Kuksanov, N.K., and Salimov, R.A., *Proc. EPAC I,* Rome, 1988, p. 1361.
5. Kazakevich, G., Burov, A., Boffo, C., Joireman, P., Saewert, G., Schmidt, C.W., and Shemyakin, A., *Preprint FERMILAB-TM-2319-AD,* 2005. http://lss.fnal.gov/archive/test-tm/2000/fermilab-tm-2319-ad.pdf
6. Shemyakin, A., Burov, A., Crawford, A.C., Dudnikov, V., Kashikhin, V., Kroc, T., Leibfritz, J., Maclachlan j., Makarov, A., McGee, M., Nagaitsev, S., Saewert, G., Schmidt, C.W., Volk, J., Warner, A., and Vostrikov, V., *Proc. EPAC VII,* Vienna, Austria, 2000, p. 1265.

7. Alinovsky, N., Batrakov, A.M., Bedareva, T.V., Bekhtenev, E.A., Belikov, O.V., Bocharov, V.N., Borodich, V.V., Bryzgunov, M.I., Bubley, A.V., Chekavinskiy, V.A., Cheskidov, V.G., Dovzhenko, B.A., Erokhin, A.I., Fatkin, G.A., Fedotov, M.G., Goncharov, A.D., Gorchakov, K.M., Gosteev, V.K., Gusev, I.A., Ivanov, A.V., Karpov, G.V., Koisin, Yu.I., Kondaurov, M.N., Kryuchkov, A.M., Lisitsyn, A.D., Lopatkin, I.A., Mamkin, V.R., Medvedko, A.S., Panasyuk, V.M., Parkhomchuk, V.V., Poletaev, I.V., Polukhin, V.A., Protopopov, A.Yu., Pureskin, D.N., Putmakov, A.A., Reva, V.B., Semenov, E.P., Senkov, D.V., Skorobogatov, D.N., and Zapiatkin, N.P., *Proc. COOL-11,* Alushta, Ukraine, 2011, p. 37.

8. Reva, V.B., Alinovskiy, N.I., Bedareva, T.V., Bekhtenev, E.A., Belikov, O.V., Bocharov, V.N., Borodich, V.V., Bryzgunov, M.I., Bubley, A.V., Chekavinskiy, V., Cheskidov, V., Dovzhenko, B., Erokhin, A., Fedotov, M., Goncharov, A.D., Gorchakov, K., Gosteev, V.K., Gusev, I., Ivanov, A., Karpov, G., Koisin, Yu., Kondaurov, M., Kozak, V., Kruchkov, A., Lisitsyn, A., Lopatkin, I., Mamkin, V., Medvedko, A.S., Panasyuk, V.M., Parkhomchuk, V.V., Poletaev, I., Polukhin, V., Protopopov, A., Pureskin, D., Putmakov, A., Selivanov, P.A., Semenov, E., Senkov, D., Skorobogatov, D.N., and Zapiatkin, N.P., *Proc. COOL-13,* Murren, Switzerland. 2013, p. 79.

9. Prandtl, L., *Essentials of Fluid Dynamics*, New York: Hafner, 1952; Moscow: InLit, 2002.

10. Abdurashitov, S.A., Tupichenkov, A.A., Vershinin, I.M., and Tenengol'ts, S.M., *Nasosy i kompressory* (Pumps and Compressors), Moscow: Nedra, 1974.

11. Alinovskii, N.I., Bulushev, A.F., Klyuev, V.F., Konstantinov, E.S., Konstantinov, S.G., Kozhemyakin, A.V., Kryuchkov, A.M., Parkhomchuk, V.V., Petrichenkov, M.V., Rastigeev, S.A., Reva, V.B., and Sukhina, B.N., *Vopr. At. Nauki Tekhn.,* 2006, no. 2, p. 34. http://vant.kipt.kharkov.ua.

12. Salimov, R.A., *Phys.-Usp.,* 2000, vol. 43, no. 2, p. 189.

13. Reginato, L., *Proc. PAC-1991,* San Francisco: 1991, p. 2918.

Translated by N. Goryacheva